



UNIVERSITY OF LEEDS

This is a repository copy of *A MUSIC-based method for SSVEP signal processing*.

White Rose Research Online URL for this paper:

<http://eprints.whiterose.ac.uk/125857/>

Version: Accepted Version

Article:

Chen, K, Liu, Q, Ai, Q et al. (3 more authors) (2016) A MUSIC-based method for SSVEP signal processing. *Australasian Physical and Engineering Sciences in Medicine*, 39 (1). pp. 71-84. ISSN 0158-9938

<https://doi.org/10.1007/s13246-015-0398-6>

© Australasian College of Physical Scientists and Engineers in Medicine 2016. This is an author produced version of a paper published in *Australasian Physical and Engineering Sciences in Medicine*. The final publication is available at Springer via <https://doi.org/10.1007/s13246-015-0398-6>. Uploaded in accordance with the publisher's self-archiving policy.

Reuse

Unless indicated otherwise, fulltext items are protected by copyright with all rights reserved. The copyright exception in section 29 of the Copyright, Designs and Patents Act 1988 allows the making of a single copy solely for the purpose of non-commercial research or private study within the limits of fair dealing. The publisher or other rights-holder may allow further reproduction and re-use of this version - refer to the White Rose Research Online record for this item. Where records identify the publisher as the copyright holder, users can verify any specific terms of use on the publisher's website.

Takedown

If you consider content in White Rose Research Online to be in breach of UK law, please notify us by emailing eprints@whiterose.ac.uk including the URL of the record and the reason for the withdrawal request.



eprints@whiterose.ac.uk
<https://eprints.whiterose.ac.uk/>

A MUSIC-based Method for SSVEP Signal Processing

Kun Chen^{1,3}, Quan Liu^{2,3,*}, Qingsong Ai^{2,3}, Zude Zhou^{1,3}, Sheng Quan Xie⁴, Wei Meng^{2,3}

¹School of Mechanical and Electronic Engineering, Wuhan University of Technology, Wuhan 430070, China

²School of Information Engineering, Wuhan University of Technology, Wuhan 430070, China

³Key Laboratory of Fiber Optic Sensing Technology and Information Processing, Ministry of Education, Wuhan 430070, China

⁴Department of Mechanical Engineering, The University of Auckland, Auckland 1010, New Zealand

*Corresponding author: email: quanliu@whut.edu.cn; Tel: +862787655520; Fax: +862787655520

1 Abstract

2 The research on brain computer interfaces (BCIs) has
3 become a hotspot in recent years because it offers benefit to
4 disabled people to communicate with the outside world.
5 Steady state visual evoked potential (SSVEP)-based BCIs
6 are more widely used because of higher signal to noise ratio
7 (SNR) and greater information transfer rate (ITR) compared
8 with other BCI techniques. In this paper, a multiple signal
9 classification (MUSIC)-based method was proposed for
10 multi-dimensional SSVEP feature extraction. 2-second data
11 epochs from four electrodes achieved excellent accuracy
12 rates including idle state detection. In some asynchronous
13 mode experiments, the recognition accuracy reached up to
14 100%. The experimental results showed that the proposed
15 method attained good frequency resolution. In most
16 situations, the recognition accuracy was higher than
17 canonical correlation analysis (CCA), which is a typical
18 method for multi-channel SSVEP signal processing. Also, a
19 virtual keyboard was successfully controlled by different
20 subjects in an unshielded environment, which proved the
21 feasibility of the proposed method for multi-dimensional
22 SSVEP signal processing in practical applications.

23 Keywords

24 brain computer interface (BCI), steady state visual evoked
25 potential (SSVEP), multiple signal classification (MUSIC),
26 feature extraction.

28 1 INTRODUCTION

29 A brain computer interface (BCI) is a communication
30 system that does not depend on the brain's normal output
31 pathways of peripheral nerves and muscles[1]. The ultimate
32 goal of a BCI is to create a specialized interface that allows
33 an individual with severe motor disabilities to have effective
34 control of devices such as computers, speech synthesizers,
35 assistive appliances and prostheses[2].

36 Electroencephalography (EEG) is most commonly used
37 for BCIs because it has advantages of portability and ease of
38 use. A steady state visual evoked potential (SSVEP) is a
39 periodic response to a visual stimulus modulated at a
40 frequency higher than 6 Hz[3] (or 4Hz[4]). It can be
41 recorded from the scalp as a nearly sinusoidal oscillatory
42 waveform with the same fundamental frequency as the
43 stimulus, and often includes some higher harmonics. The
44 amplitude and phase characteristics of SSVEPs depend upon
45 the stimulus intensity and frequency. SSVEP-based BCIs are
46 becoming a research hotspot because it has many advantages

47 over other BCI systems including a higher signal to noise
48 ratio (SNR), and faster information transfer rate (ITR). It
49 also does not require intensive training [5].

50 A variety of methods have been developed and used for
51 feature extraction for SSVEP-based BCIs[6]. Fourier-based
52 transform methods are mostly used for power spectrum
53 density analysis (PSDA). Most research used them to
54 compute the accumulative power at the stimulus frequencies
55 and their harmonics for frequency-coded SSVEPs. Or the
56 average power centered on the stimulus frequency was
57 calculated[7]. An important advantage of Fourier-based
58 transforms is their simplicity and small computation time.
59 However, the time window length of SSVEP signals needs to
60 be long enough to enhance the frequency resolution of FFT
61 when the sampling frequency is confirmed. This might limit
62 practical applications because it has a lower information
63 transfer rate (ITR) [8]. Additionally, a larger window length
64 could lead to classification errors during the changing of
65 stimuli. The studies [8-10] all used wavelet analysis to
66 estimate power at relevant frequency points. A key problem
67 with applying wavelet analysis is how to choose an
68 appropriate mother wavelet to attain good performance.
69 Although the wavelet analysis is better for non-stationary
70 signal processing compared with Fourier transform, it is
71 developed based on Fourier transform, which is fit for
72 processing linear signals. New methods suitable for
73 non-linear and non-stationary signal processing are needed.
74 In this case, Hilbert Huang transform (HHT) is adopted in
75 previous studies [11,12]. HHT has more stability than FFT,
76 which means the recognition accuracy will not change
77 greatly when the data length varies. Although HHT can be
78 well used for non-linear and non-stationary SSVEPs, its
79 computation time is higher compared with Fourier transform.
80 All the methods discussed above were commonly employed
81 to process single channel SSVEPs. Signals from
82 multi-channel EEG are less affected by noise than signals
83 from a unipolar or bipolar system. The combination of
84 signals collected from different channels (electrodes) is also
85 referred to as spatial filtering. Typical methods like
86 minimum energy combination (MEC) and maximum
87 contrast combination (MCC) are the most commonly utilized
88 [13-16]. Another method named canonical correlation
89 analysis (CCA) can be employed to extract features from a
90 different viewpoint. It computes the correlation of two
91 multi-variable datasets [17]. Paper [18] used CCA to
92 recognize SSVEP for the first time. A further comparison
93 between the CCA and PSDA method was done by Hakvoort

94 et al. [19], which showed that CCA had better performance.
 95 Spatial filtering methods have the advantage of combining
 96 signal pre-processing and feature extraction together.

97 In this paper, a new method based on multiple signal
 98 classification (MUSIC) was proposed for feature extraction
 99 of multi-dimensional SSVEPs. One of the typical
 100 applications of MUSIC is to solve the problem of harmonic
 101 retrieval for one-dimensional signals. The principle of using
 102 MUSIC for target frequency recognition of
 103 multi-dimensional SSVEPs was explained in detail. Also, a
 104 criterion used to determine the number of eigenvectors
 105 constructing the signal subspace for power spectrum
 106 estimation was proposed. The method was verified with both
 107 simulated and real SSVEP data. Experiments in synchronous
 108 and asynchronous modes were conducted. The results show
 109 that MUSIC achieved a good frequency resolution.
 110 Meanwhile, it is capable of suppressing noise because it
 111 decomposes the original data into signal subspace and noise
 112 subspace. Compared with CCA, MUSIC is more flexible, as
 113 the number of eigenvectors constructing the signal subspace
 114 is adjustable. The recognition accuracy was better than CCA
 115 in most situations. Finally, the proposed method was
 116 successfully utilized for users to control a virtual keyboard in
 117 an unshielded environment.

118 This paper is organized as follows: methods including the
 119 principle of MUSIC, the procedure of SSVEP signal
 120 processing and the setup of experiments are explained in
 121 Section 2. The experimental results are illustrated in Section
 122 3. Discussion and conclusions are presented in Section 4 and
 123 Section 5.

124 2 MATERIALS AND METHODS

125 2.1 Multiple Signal Classification for SSVEP Signal 126 Processing

127 MUSIC was first proposed by R. O. Schmidt in 1979[20].
 128 It is often used to solve the problem of harmonic retrieval
 129 and direction of arrival. The data model [21] can be
 130 expressed as follows.

$$131 \quad x(n) = \sum_{k=1}^p a_k \exp(j2\pi n f_k + j\phi_k) + w(n) \quad (1)$$

132 Here, $w(n)$ is additive noise. a_k , f_k and ϕ_k represent the
 133 amplitude, frequency and phase respectively. p denotes the
 134 number of harmonics.

135 The SSVEP signal is a periodic response to the stimulus
 136 frequency and its harmonics, which can be modeled using
 137 the above formula. Actually, many other methods like MEC,
 138 MCC or CCA employ similar data models to represent
 139 SSVEPs. The model includes sum of stimulus frequencies
 140 and noise. They are typically used for multi-channel signals.
 141 In this situation, the data model should be defined as:

$$142 \quad \mathbf{XX}(n) = [x_1(n), x_2(n), \dots, x_{\text{num}}(n)] \quad (2)$$

143 Here, num is the number of channels. It is assumed that the
 144 data includes both signals and noises, which are independent
 145 of each other[22]. Thus, the covariance matrix can be
 146 decomposed into signal and noise components.

147 As mentioned before, the typical use of MUSIC method is

148 to solve the problem of harmonic retrieval for
 149 one-dimensional signals. The principle of using MUSIC for
 150 multi-dimensional SSVEP signal processing is illustrated as
 151 follows.

152 A simulated signal according to Formula (1) is generated
 153 as:

$$154 \quad x(n) = 0.5 * \sqrt{20} * \sin(2\pi * 5.384 * n / f_s) + \quad (3)$$

$$155 \quad \sqrt{10} * \sin(2\pi * 5.871 * n / f_s) + 15.5 * \text{randn}(1,512)$$

156 Where, the value of f_s is 256, and n ranges from 1 to
 157 512. It can be seen that there are two harmonic components
 158 with frequencies of 5.384 Hz and 5.871 Hz for the simulated
 159 signal. The spatial smoothing method which reconstructs
 160 one-dimensional signals to multi-dimensional signals, is
 161 usually employed to analyze the signal as Formula (3). The
 162 reconstructed signal is an $N \times M$ dimension matrix. As for
 163 the MUSIC method, N means the number of snapshots, and
 164 M means the number of arrays. The reconstructed
 multi-dimensional signal can be represented by a matrix X .

$$165 \quad X = \begin{bmatrix} x(1) & x(2) & \dots & x(M) \\ x(2) & x(3) & \dots & x(M+1) \\ \dots & \dots & \dots & \dots \\ x(N) & x(N+1) & \dots & x(M+N-1) \end{bmatrix} \quad (4)$$

166 The first row of the new matrix includes
 167 $x(1), x(2), \dots, x(M-1), x(M)$; the second row of the new
 168 matrix includes $x(2), x(3), \dots, x(M), x(M+1)$, and so on.
 169 The last row includes
 170 $x(N), x(N+1), \dots, x(M+N-2), x(M+N-1)$. Because the
 171 total number of sampling points for the original signal $x(n)$
 172 is 512, the maximum sum of M and N is 513.

173 The values of M and N were adjusted to reconstruct the
 174 signal. The result of power spectral analysis for the new
 175 multi-dimensional signal with various values of M and N
 176 is illustrated as Fig. 1.

177 It is seen in Fig. 1(a) only one harmonic component of
 178 5.632 Hz is recognized. While in Fig. 1(b), Fig. 1(c) and Fig.
 179 1(d), two harmonic components of 5.376 Hz and 5.888 Hz
 180 can be recognized, which are quite close to the harmonic
 181 components of the original signal represented by Formula
 182 (3). For real SSVEP signals, the recognition accuracy of
 183 target frequencies doesn't normally need to be 0.001 Hz. The
 184 harmonic recognition effect became better with the value of
 185 M increasing in experiments. However, the result would
 186 not improve any more if M increased to some extent.

187 For the matrix X , each row can be seen as a time series.
 188 Compared the next row with the last row, the next one can be
 189 regarded as a unit-time delay time series of the last one. The
 190 real SSVEP signal as in Formula (2) can be also represented
 191 by a matrix \mathbf{XX}_{new} .

$$192 \quad \mathbf{XX}_{\text{new}} = \begin{bmatrix} x_1(1) & x_1(2) & \dots & x_1(\text{sam}) \\ x_2(1) & x_2(2) & \dots & x_2(\text{sam}) \\ \dots & \dots & \dots & \dots \\ x_{\text{num}}(1) & x_{\text{num}}(2) & \dots & x_{\text{num}}(\text{sam}) \end{bmatrix} \quad (5)$$

193 sam means the sampling points, and num denotes the
 194 number of electrodes (channels). Each row of XX_{new} is also
 195 a time series. For electrodes are laid at different positions,
 196 the time series according to each electrode might be regarded
 197 as signals with different transmitting distances from the
 198 same sources. It means for XX_{new} , the next row can be
 199 regarded as a time-delay series of the last one. From this

200 perspective, XX_{new} as in Formula (5) and X in Formula (4)
 201 are quite similar. XX_{new} can be seen as the reconstructed
 202 multi-dimensional signal, which is to be analyzed by the
 203 MUSIC method for harmonic components recognition. The
 204 feasibility of using MUSIC for multi-dimensional SSVEP
 205 signal processing were verified by both simulated data and
 206 real SSVEP data, and it can be seen in the section Results.

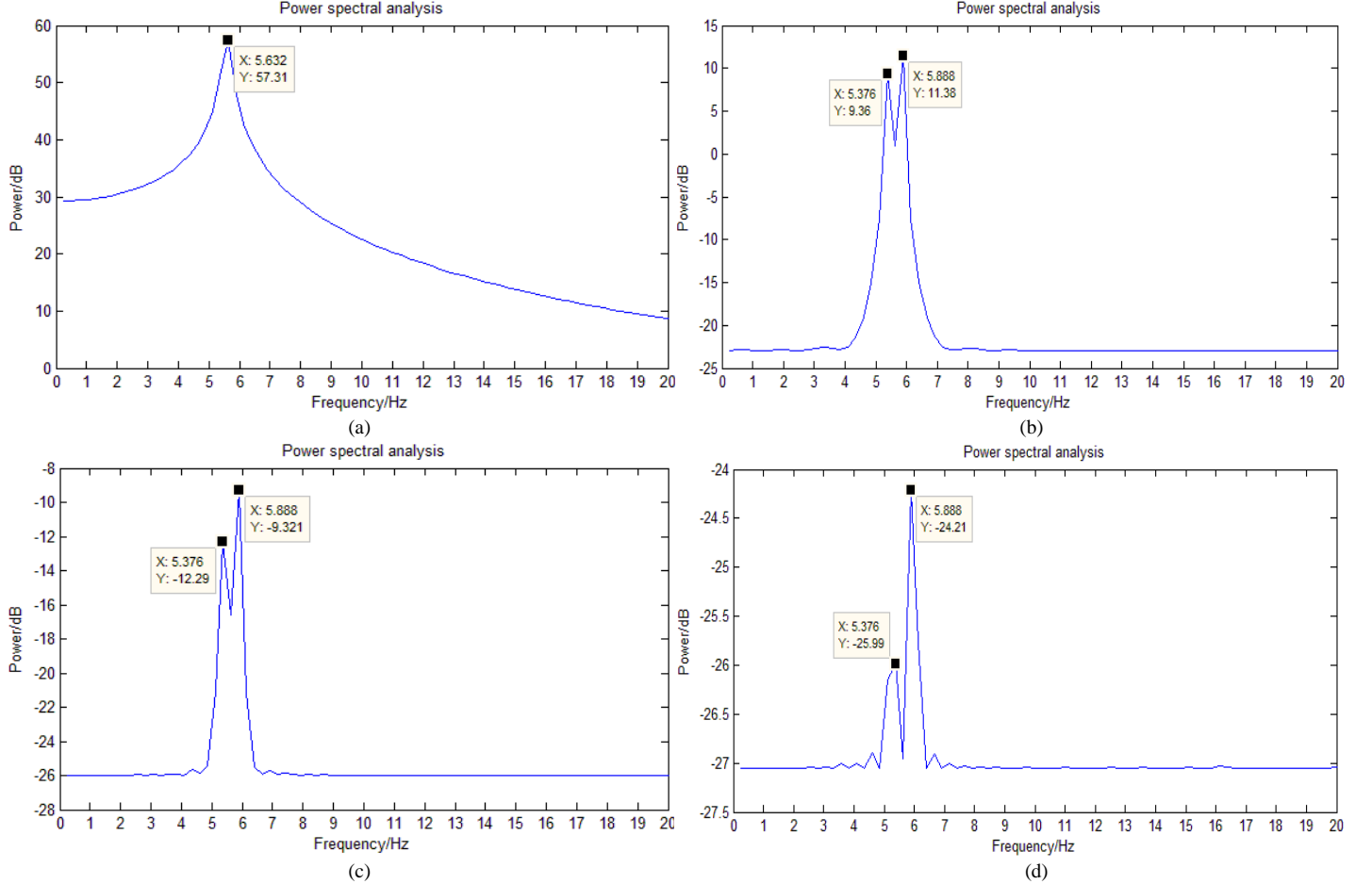


Fig. 1 Power spectral analysis for reconstructed signal with various values of M and N . (a) $M=5, N=507$; (b) $M=200, N=312$;
 (c) $M=500, N=12$; (d) $M=508, N=4$.

213 The detailed computation procedure is described as
 214 follows:

215 (1) Assume that the original SSVEP signal is a $sam \times num$
 216 dimension matrix. sam and num represent the number of
 217 sampling points and the number of channels.

218 (2) As explained above, sam can be seen as M in
 219 Formula (4), and num can be seen as N . The covariance
 220 matrix R_{XX} of the new matrix XX_{new} is a $sam \times sam$
 221 dimensional matrix. Compute the eigenvalues $d_1, d_2, \dots,$
 222 d_{sam} and eigenvectors V_1, V_2, \dots, V_{sam} of the covariance
 223 matrix.

224 (3) The eigenvectors corresponding to the k largest
 225 eigenvalues constitute the signal subspace, while the
 226 remaining eigenvectors constitute the noise subspace. How
 227 to confirm the value of k is also discussed in this paper.

228 (4) Use the signal subspace or the noise subspace for power
 229 spectrum estimation as follows.

230 spectrum estimation as follows.

$$231 \quad P(f) = 1 / (a_F (I - S_i S_i^T) a_F^T) \quad (6)$$

$$232 \quad P(f) = 1 / (a_F^T (N_o N_o^T) a_F) \quad (7)$$

233 I is a $sam \times sam$ dimensional unit matrix. S_i and
 234 N_o represent the signal and the noise subspace with
 235 dimensions of $sam \times k$ and $sam \times (sam - k)$. a_F is a
 236 $1 \times sam$ dimensional matrix. The value of each element is:

$$237 \quad a_F(l, i) = e^{-j^{*(i-1)*\varpi_{order}}, i \in (1, 2, \dots, sam) \quad (8)$$

$$238 \quad order = round(f / \Delta f) + 1 \quad (9)$$

$$239 \quad \varpi_{order} = 2 * \pi * \Delta f * order / f_s \quad (10)$$

240 Here, f_s is the sampling frequency, Δf is the frequency
 241 interval, and f is the target frequency..

242 The value of k can be defined as a constant which is
 243 obtained by conducting experiments. The idea is like setting

244 a threshold. It needs time to adjust the value to maximize the
 245 recognition results. Inspired by the principle of minimum
 246 energy combination [14], which is another important
 247 technique for spatial filtering, the number of eigenvalues is
 248 chosen corresponding to the following equation.

$$249 \quad d_i / d_1 > 0.01, i = 1, 2, 3, \dots, k \quad (11)$$

250 Here, d_1 is the largest eigenvalue of the covariance matrix
 251 and d_1, d_2 till d_k are sorted in descending order. Only
 252 these eigenvectors whose corresponding eigenvalues are no
 253 less than 1% of the largest eigenvalue are classified as the
 254 signal subspace for spectrum estimation.

255 The SSVEP signal processing usually includes data
 256 pre-processing, feature extraction and feature classification.
 257 In our research, a low-pass filter with a cut-off frequency of
 258 30 Hz and a 50 Hz notch filter were used for pre-processing.
 259 The original data were segmented into epochs for feature
 260 extraction via the MUSIC method. The basic idea is to
 261 compute the power values at stimulus frequencies. As for
 262 feature classification, the frequency corresponding to the
 263 maximum power value was recognized as the target one. If
 264 there are n stimulus frequencies which are f_1, f_2 till f_n .
 265 The power value $P(f)$ corresponding to each frequency is
 266 computed as shown in Formula (6). And then the target
 267 frequency is confirmed as the following formulas.

$$268 \quad f_{\text{target}} = \arg \max (P(f)) \quad (12)$$

$$269 \quad t \text{ arg et} \in \{1, 2, \dots, n\} \quad (13)$$

270 From the above two formulas, it can be seen that we should
 271 focus on the magnitude relation of power values
 272 corresponding to different stimulus frequencies, not the
 273 absolute magnitude of a specific power value. Therefore, the
 274 units of power values are not labeled in all figures in this
 275 paper.

276 A dwell time, which means the state of one target kept for
 277 a period of time, was employed to reduce the false positives.
 278 The detailed explanations about this are given in the Results
 279 and Discussion sections.

280 The recognition results were compared with the CCA
 281 method in experiments. Here, the principle of CCA[23] is
 282 briefly introduced. If there are two variables X and Y with
 283 dimensions of p and q respectively. X and Y are
 284 represented as $X = (X_1, X_2, \dots, X_p)$ and $Y = (Y_1, Y_2, \dots, Y_q)$.

285 To find out the relation between X and Y , a linear
 286 combination is applied to both X and Y . Two new
 287 variables are generated which are
 288 $U = a_1 X_1 + a_2 X_2 + \dots + a_p X_p$ and
 289 $V = b_1 Y_1 + b_2 Y_2 + \dots + b_q Y_q$. Then the correlation coefficient
 290 $\rho = \text{corr}(U, V)$ between U and V is computed.

291 $a = (a_1, a_2, \dots, a_p)$ and $b = (b_1, b_2, \dots, b_q)$ are named
 292 canonical variables when p has the largest value, and ρ is
 293 the canonical correlation coefficient between X and Y .

294 If there are four stimulus frequencies used in practical
 295 applications which are f_1, f_2, f_3 and f_4 , four reference

296 signals should be constructed as follows:

$$297 \quad X_{21} = \begin{bmatrix} \sin(2\pi * f_1 * t) \\ \cos(2\pi * f_1 * t) \end{bmatrix} \quad (14)$$

$$298 \quad X_{22} = \begin{bmatrix} \sin(2\pi * f_2 * t) \\ \cos(2\pi * f_2 * t) \end{bmatrix} \quad (15)$$

$$299 \quad X_{23} = \begin{bmatrix} \sin(2\pi * f_3 * t) \\ \cos(2\pi * f_3 * t) \end{bmatrix} \quad (16)$$

$$300 \quad X_{24} = \begin{bmatrix} \sin(2\pi * f_4 * t) \\ \cos(2\pi * f_4 * t) \end{bmatrix} \quad (17)$$

301 If the original SSVEP data are denoted by X_1 , the
 302 aforementioned CCA method is used to compute the
 303 correlation coefficients $\rho_1, \rho_2, \rho_3, \rho_4$ between X_1 and
 304 $X_{21}, X_{22}, X_{23}, X_{24}$. Then the target frequency is
 305 determined according to the following formula.

$$306 \quad f_{\text{target}} = \arg \max (\rho(f)), t \text{ arg et} \in \{1, 2, 3, 4\} \quad (18)$$

307 It is noted that the reference signals only use the
 308 fundamental harmonic components corresponding to
 309 stimulus frequencies. The second or other harmonics can be
 310 also used to calculate the correlation coefficients if
 311 necessary.

312 2.2 Experimental Setup

313 As the signal and noise components of simulated data are
 314 deterministic, the simulated data are suitable for method
 315 verification. But the real SSVEP data are more persuasive to
 316 prove that the proposed method can be used in practical
 317 applications. So both simulated and real SSVEP data were
 318 used in our experiments.

319 1) Simulated data

320 In experiments, four-channel data were generated. Each
 321 channel includes two sine waves to simulate the harmonic
 322 components of SSVEP and random noise. The frequencies of
 323 two sine components are 5.384 and 5.871 Hz, respectively,
 324 just like the harmonic components used in Formula (19). The
 325 data are expressed as follows.

$$326 \quad S = [S_1; S_2; S_3; S_4] = \begin{bmatrix} 0.5 * \sqrt{20} * \sin(2\pi * 5.384 * n / f_s) + \\ \sqrt{10} * \sin(2\pi * 5.871 * n / f_s) + 15.5 * \text{randn}(1, N); \\ 0.1 * \sqrt{20} * \sin(2\pi * 5.384 * n / f_s) - \\ 0.8 * \sqrt{10} * \sin(2\pi * 5.871 * n / f_s) + 15.5 * \text{randn}(1, N); \\ 0.2 * \sqrt{20} * \sin(2\pi * 5.384 * n / f_s) + \\ \sqrt{10} * \sin(2\pi * 5.871 * n / f_s) + 15.8 * \text{randn}(1, N); \\ 0.1 * \sqrt{20} * \sin(2\pi * 5.384 * n / f_s) + \\ \sqrt{10} * \sin(2\pi * 5.871 * n / f_s) + 16.5 * \text{randn}(1, N) \end{bmatrix} \quad (19)$$

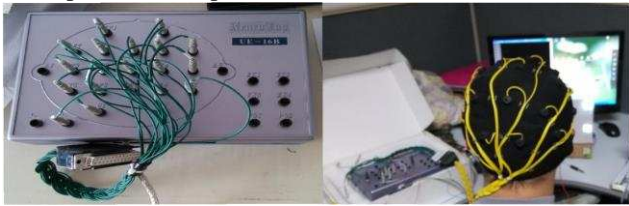
327 Here, f_s is the sampling frequency equal to 256 Hz. N is
 328 the total number of sampling points with a value of 512. n
 329 represents each single sampling point ranging from 1 to 512.
 330 Thus, S is a 4×512 dimensional matrix. It is noticed that the

332 frequency interval of two components is 0.487 Hz. It doesn't
 333 strictly meet the frequency resolution requirement for
 334 traditional FFT method to estimate the spectrum, because the
 335 resolution is computed as 0.5 Hz ($f_s / N = 256 / 512$). Also,
 336 both of the frequency points 5.384 and 5.871 are not located
 337 on the FFT spectral lines. However, MUSIC can better
 338 estimate the power values at these two points. It is shown in
 339 the Results section.

340 2) Real SSVEP data

341 The stimulus panel contains four LED blocks each
 342 measured as 2*2 cm. The distance between LED blocks and
 343 the flickering frequencies are adjustable. The effects of these
 344 parameters on experimental results are discussed in the
 345 following section.

346 A Symtop UE-16B EEG amplifier was used in our
 347 experiments as shown in Fig. 2. It has 16 channels and a USB
 348 interface. The maximum sampling frequency can be adjusted
 349 to 1000 Hz. A low-pass filter and a notch filter are
 350 developed in the amplifier.

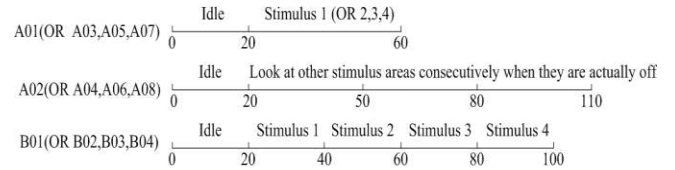


351 **Fig. 2** UE-16B EEG amplifier and the experimental setup

352 In reality, the sampling frequency was set to 200 Hz,
 353 because the frequency of EEG signals is usually lower than
 354 100 Hz. Also, the stimuli frequencies used in experiments
 355 are lower than 30 Hz. The choice of 200 Hz is reasonable.
 356 Besides, an appropriate sampling frequency rather than a
 357 higher frequency saves the computation time. The cut off
 358 frequency of the low-pass filter was set to 30 Hz and the 50
 359 Hz power line interference was removed by a notch filter.
 360 All 16 channels (Fp1, Fp2, F3, F4, C3, C4, P3, P4, O1, O2,
 361 F7, F8, T3, T4, T5, and T6) were utilized to acquire the
 362 original EEG data in early stages. The number of channels
 363 was reduced to 4 (P3, P4, O1, O2) in later experiments. **Five**
 364 **subjects (one female, four male) participated in the**
 365 **experiments for performance analysis of related methods.**
 366 **All of them have good eye vision. The average age is 25.4**
 367 **years old. More subjects were asked to conduct the**
 368 **experiment for real time control of a virtual keyboard. All**
 369 **experiments were done in an unshielded environment.**

370 Two different kinds of experiments were designed for the
 371 five subjects, namely synchronous paradigm and
 372 asynchronous paradigm. **Regarding the synchronous one,**
 373 **three sessions were conducted: (i) Only one of the four**
 374 **stimuli was flickering. Subjects looked at the flickering one**
 375 **for 40 seconds from the 20th second; (ii) Only one of the four**
 376 **stimuli was flickering. Subjects looked at each area**
 377 **corresponding to stimuli not flickering for 20 seconds**
 378 **consecutively from the 20th second; (iii) Four stimuli were**
 379 **flickering at the same time. Subjects looked at each one for**
 380 **20 seconds consecutively from the 20th second. Labels were**

383 used to indicate different experiment sessions as illustrated
 384 in Fig. 3. As for the asynchronous paradigm, two following
 385 sessions were carried out: (i) Subjects looked at different
 386 stimuli according to a predefined number sequence. Once a
 387 target was recognized, subjects turned to look at the next
 388 stimulus. In our experiments, three number sequences were
 389 defined as '1-2-3-4', '1-3-2-4' and '1-4-2-3'; (ii) Subjects
 390 looked at stimuli randomly, and no sequence was defined
 391 before the experiment.



392 **Fig. 3** Explanation of SSVEP dataset labels in the synchronous mode

393 3) Virtual keyboard layout

394 In order to verify the aforementioned method, a virtual
 395 keyboard was designed for subjects to input words. In this
 396 application, four stimuli were used to move the cursor along
 397 four different directions: up, down, left and right. The fifth
 398 stimulus was used to represent the "confirm" command for
 399 selecting a letter or a symbol of the keyboard. It can be seen
 400 from Fig. 4 that the keyboard contains 26 letters and other
 401 symbols. The layout of the keyboard is based on the
 402 frequency of how often these symbols are used [14]. The
 403 more frequent they are used, the closer they are placed near
 404 the center of the keyboard. When the cursor moved on a
 405 letter or a symbol, the background color turns red. When the
 406 letter or the symbol is selected, the text box at the bottom of
 407 the screen displays the selected symbol with previous
 408 symbols.

409 3 RESULTS

410 3.1 Simulated Data Analysis

411 Fig. 5(a) illustrates the power spectrum obtained by
 412 MUSIC method. The spectrum area around 6 Hz was
 413 zoomed in as shown in Fig. 5(b).

414 It is obvious in Fig. 5(b) that two peaks appear at around
 415 5.3 and 5.8 Hz, which are almost equal to the harmonic
 416 components of the simulated data. Also, the spectral curve is
 417 smooth in Fig. 5(b), which means a high frequency
 418 resolution can be acquired.

419 3.2 Real SSVEP Data Analysis

420 For real SSVEP signals, MUSIC was utilized to calculate
 421 the power at those stimulus frequency points. The stimulus
 422 frequency corresponding to the maximum power value was
 423 recognized as the target one. Taking the processing results of
 424 dataset A03 as an example, as shown in Fig. 6, four curves
 425 with different colors represent the power values of the four
 426 stimulus frequencies (6, 7, 8, 9 Hz). The values
 427 corresponding to the second stimulus are higher than the
 428 other three after the 22nd seconds. The 2-second delay is
 429 mainly caused by the response time when subjects changed
 430 from the idle state to the work state. In addition, a dwell time,

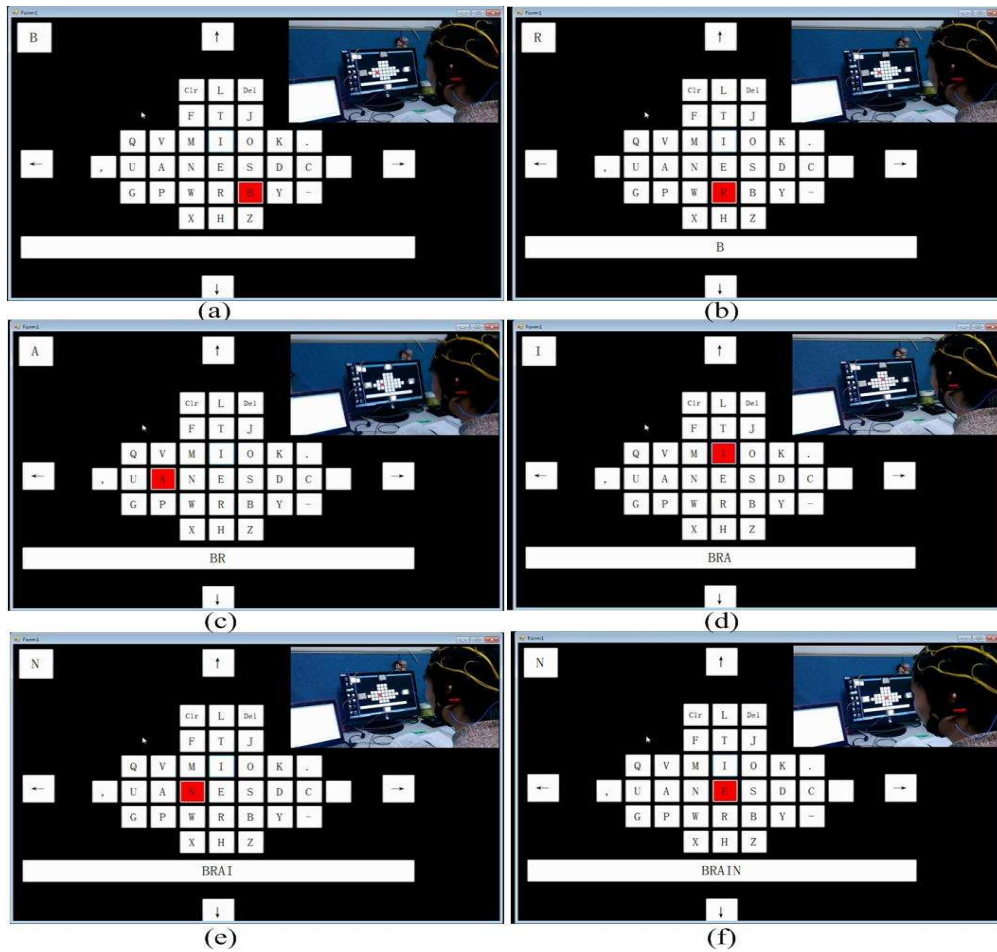


Fig. 4 Control of a virtual keyboard based on SSVEP

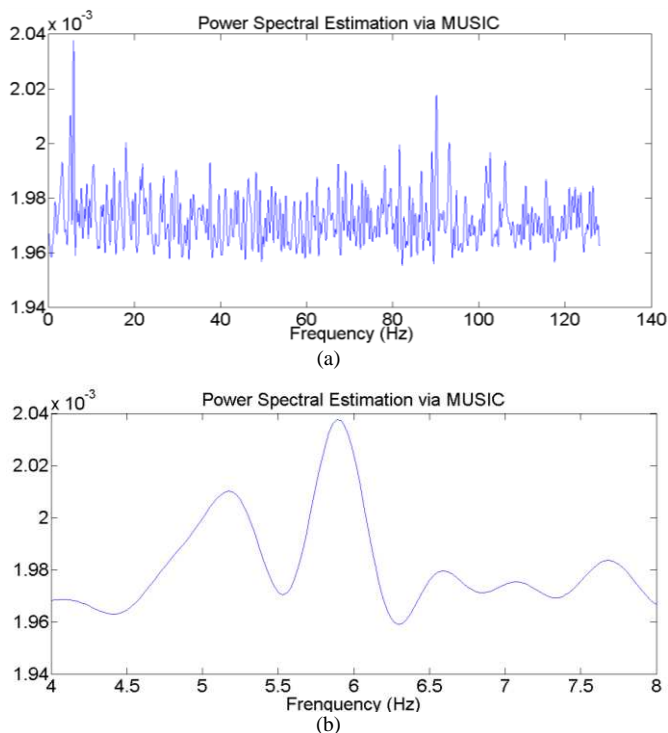


Fig. 5 Spectrum of the simulated data computed by MUSIC

444 applications in order to reduce the false positives. The dwell
 445 time was adjusted in experiments. The CCA method was
 446 used to compare the processing results. The original SSVEP
 447 data were segmented into epochs of 400 sampling points,
 448 which means the time duration was 2 seconds (sampling
 449 frequency is 200 Hz). Data overlapping was used to make
 450 the time window move smoothly. Results of no overlapping
 451 and 50% overlapping were compared.

452 Table 1 shows one subject's recognition rates under
 453 different conditions during the first session in the
 454 synchronous mode. The frequencies corresponding to A01,
 455 A03, A05 and A07 were 6, 7, 8 and 9 Hz. Original data were
 456 segmented into epochs of 400 points.

457 The recognition rates of one subject during the second
 458 session are shown in Table 2. In this session, only one
 459 stimulus was flickering. The subjects looked at other areas of
 460 stimuli not flickering in order, which means the subjects
 461 were in idle states all the time. So, the aforementioned dwell
 462 time was utilized. Several consecutive decisions made one
 463 final target choice. The parameter of consecutive numbers
 464 was tested in experiments. Overlapping was also employed
 465 to recognize the target smoothly.

433
 434
 435
 436
 437
 438
 439
 440
 441
 442 which means SSVEP signals responding to one stimulus
 443 have to keep for a period of time, was employed in real

Frequency power estimation via MUSIC

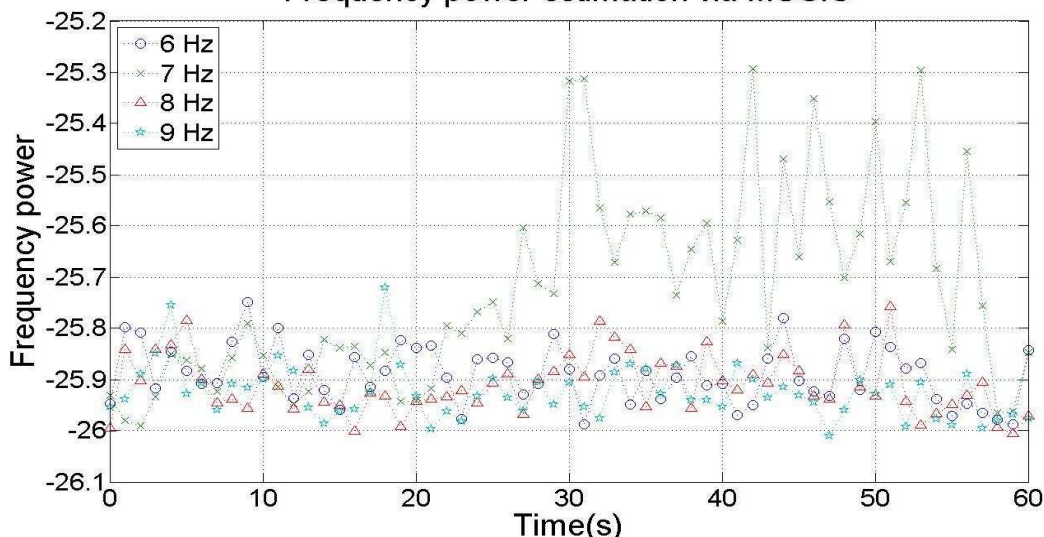


Fig. 6 Frequency power estimation corresponding to dataset A03

466
467
468

In the third session, the use of covers on stimuli, the distance of neighboring stimuli were changed to compare the different recognition results. The four stimulus frequencies used in Table 3 were 6.5, 7.5, 8.5 and 9.5 Hz, respectively.

Table 1 Recognition rates under different conditions during the first session in the synchronous mode[24]

Conditions *		1	2	3
A01	MUSIC	0.8571	0.9024	0.7073
	CCA	0.7619	0.8293	0.6829
A03	MUSIC	0.8571	0.878	0.9268
	CCA	0.7619	0.8293	0.9268
A05	MUSIC	0.8571	0.878	0.9268
	CCA	0.7143	0.878	0.8537
A07	MUSIC	0.8571	0.8537	0.9268
	CCA	0.8095	0.8293	0.9024

* Condition 1: data length=400, overlapping=0; number of channels=16;
Condition 2: data length=400, overlapping =50%; number of channels=16;
Condition 3: data length=400, overlapping =50%; number of channels=4.

In the first session of the asynchronous mode, subjects looked at stimuli following predefined number sequences '1-2-3-4', '1-3-2-4' and '1-4-2-3'. Once a target was recognized, subjects turned to look at another one immediately. It is different from the experiments in the synchronous mode, in which subjects looked at each stimulus for a fixed period of time.

Table 2 Recognition rates under different conditions during the second session in the synchronous mode[24]

Conditions*		1	2	3	4
A02	MUSIC	0.6607	0.5495	0.7928	0.8908
	CCA	0.5	0.5135	0.6937	0.8829
A04	MUSIC	0.6429	0.5315	0.7838	0.8288
	CCA	0.6429	0.6126	0.8108	0.8198
A06	MUSIC	0.7679	0.5856	0.8378	0.8829
	CCA	0.6429	0.6667	0.8559	0.9099
A08	MUSIC	0.75	0.6937	0.9279	0.8649
	CCA	0.75	0.5676	0.8288	0.8198

* Condition 1: data length=400, overlapping =0; number of channels=16; 2 consecutive decisions (overlapping: 1) made one final target choice;
Condition 2: data length=400, overlapping =50%; number of channels=16; 2 consecutive decisions (overlapping: 1) made one final target choice;
Condition 3: data length=400, overlapping =50%; number of channels=16; 3 consecutive decisions (overlapping: 2) made one final target choice;
Condition 4: data length=400, overlapping =50%; number of channels=4; 3 consecutive decisions (overlapping: 2) made one final target choice.

Table 3 Recognition rates during the third session in the synchronous mode[24]

Conditions	MUSIC	CCA
Far distance (8 cm), no use of covers	0.8025	0.8148
Far distance (8 cm), use of covers	0.8148	0.8025
Near distance (4 cm), no use of covers	0.7901	0.7531
Near distance (4 cm), use of covers	0.8148	0.8148

Frequency power estimation via MUSIC

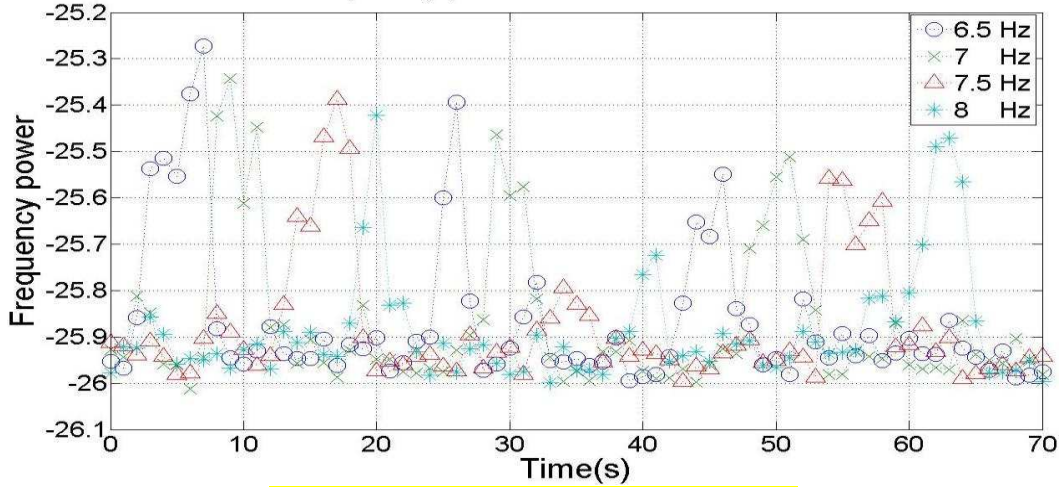


Fig. 7 Frequency power estimation in the asynchronous mode

Taking one number sequence ‘1-2-3-4’ as an example, the frequency power at four stimulus frequencies was illustrated in Fig. 7. Subjects repeated looking at stimuli orderly three times. The frequencies used were 6.5, 7, 7.5 and 8 Hz, respectively. It means the frequency resolution was reduced to 0.5 Hz, while the above experimental results were obtained with frequency resolution of 1 Hz. As seen in Fig. 7, frequencies with an interval of 0.5 Hz can be clearly distinguished using the MUSIC method just like the simulated data.

Five subjects participated in experiments. Each of them finished looking at all stimuli corresponding to three number sequences for three times. The experimental time consumption for all subjects to complete different tasks is listed in the following Table 4.

Table 4 Time consumption (seconds) during the first session in the asynchronous experimental mode

Subjects	Number sequences (repeating three times for each)		
	‘1-2-3-4’	‘1-3-2-4’	‘1-4-2-3’
Subject 1	57	57	57
Subject 2	58	59	63
Subject 3	57	51	55
Subject 4	57	58	61
Subject 5	60	62	59

Table 5 Recognition accuracy when subjects looked at stimuli randomly

Subjects	Accuracy	Total time (seconds)
Subject 1	1.0000	100
Subject 2	1.0000	103
Subject 3	0.9523	100
Subject 4	1.0000	101
Subject 5	0.9048	102

In the second session of the asynchronous mode, subjects looked at whichever stimulus as they would like to for about 100 seconds. This situation is more like the real world

applications without external interference. The first session was to estimate the time consumption time of target recognition, while this one was to estimate the recognition accuracy in the asynchronous mode as seen in Table 5.

3.3 SSVEP-based Virtual Keyboard

Fig. 4 illustrates the whole procedure of spelling the word ‘BRAIN’. For five different subjects, the time consumption of spelling ‘BRAIN’ or ‘BCI TEST’ was recorded as shown in Table 6.

Table 6 shows the spelling speed for different subjects were not the same even for the same word. As for ‘BRAIN’, it takes 11.6 to 17 seconds to output a letter or a symbol. In terms of ‘BCI TEST’, the average time is 15 to 15.88 seconds. Taking the word ‘BRAIN’ as an example, the steps of choosing these five letters starting from the keyboard center are 2, 1, 2, 1 and 1, respectively. The total step is 7. Considering the five ‘confirm’ commands, 12 steps are needed to spell the word ‘BRAIN’. It means each step takes about 4.83 to 7.08 seconds. This time is longer than that of the asynchronous mode experiments without device control. It is partly because subjects need time to choose which the next target is when spelling a specific word.

Table 6 Time consumption for different subjects of spelling different words

Subjects	Words	Time (Seconds)
Subject 1	BRAIN	58
Subject 2	BRAIN	68
Subject 3	BCI TEST	120
Subject 4	BCI TEST	127
Subject 5	BRAIN	85

4 DISCUSSION

4.1 Enhancement of Frequency Resolution

For simulated data, the MUSIC method was used to estimate the power at two nearby frequencies. As for FFT, power values can be computed only at points where the frequency is an integer multiple of the frequency resolution,

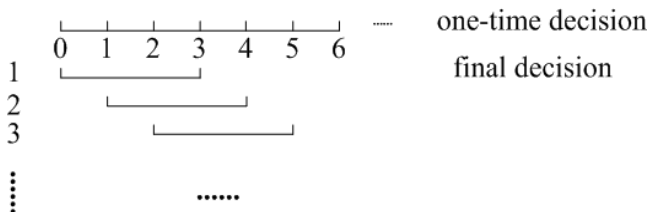
563 such as, 0, 0.5, 1, 1.5 Hz and so on. In Fig. 5(b), it is obvious
 564 that two maxima appear at around 5.3 and 5.8 Hz, which are
 565 the real harmonic components of the stimulated data. That
 566 means the MUSIC method can achieve high frequency
 567 resolution. In addition, MUSIC decomposes data into signal
 568 subspace and noise subspace. The noise can be removed to
 569 some extent when estimating the power spectrum.

570 4.2 One-target Recognition

571 For the real SSVEP signals, we compared the
 572 experimental results of MUSIC and another typically used
 573 method CCA. As shown in Tables 1-3, the MUSIC method
 574 achieved higher recognition accuracy in most cases.
 575 Exceptions existed, as the numbers in red color in these
 576 tables illustrated that CCA performed better than MUSIC
 577 sometimes.

578 In Table 1, one subject looked at only one stimulus for 40
 579 seconds. All segmented data length was 2 seconds. The
 580 accuracy was better when 50% data overlapping was used
 581 for 16-channel SSVEP signals. Also, the results showed that
 582 4-channel (P3, P4, O1 and O2) signals could be utilized for
 583 detecting the target stimulus except dataset A1. This is
 584 because not all frequencies evoke strong SSVEPs when
 585 applied to different individuals. It is proved that more
 586 channels do not definitely produce better results, because
 587 SSVEP signals are not evenly distributed on the brain
 588 surface. Some channels might contain more noise rather
 589 than SSVEP related signals. In addition, reducing the
 590 number of channels shortens the preparation time before
 591 experiments, which is important for implementing a real BCI
 592 system.

593 4.3 Idle State Detection



594
595 **Fig. 8** A dwell time used for final decisions
596

597 The frequency with the maximum power value was
 598 recognized as the target one in Table 1. However, in the idle
 599 state, when subjects didn't focus on any stimulus, this
 600 method could cause false positives. Idle state detection
 601 becomes another key issue. There are two common ways to
 602 solve this problem. A dwell time or a threshold can be
 603 employed for idle state detection. The accuracy in Table 2
 604 was calculated by using a dwell time. A same target was
 605 recognized for several consecutive times, and then a final
 606 decision was made as seen in Fig. 8. Fig. 8 shows that three
 607 consecutive decisions make a final decision, which means if
 608 three consecutive one-time decisions are identical, and then a
 609 final decision is made to confirm a target. The overlapping
 610 percentage is 2/3 in this example. That means there is a
 611 'decision window' moving along the time axis. It can be seen
 612 in Table 2 that under condition 4, where the data length was

613 400 points with 50% overlapping and the number of
 614 channels was 4, better performance was achieved than other
 615 conditions.

616 For comparison, the threshold method was also employed.
 617 The threshold was obtained from training data. For each
 618 stimulus frequency, a period time of data in the work state
 619 and the idle state was acquired. The threshold was adjusted
 620 to maximize the total recognition rate, which was defined as
 621 value of the sum of true positives and true negatives divided
 622 by the total training number.

623 As seen in Table 7, the idle state could be better detected
 624 by using a threshold. If the threshold and the dwell time were
 625 used together, the recognition accuracy can be even up to
 626 100%, such as dataset A06. It is noticed that using a
 627 threshold can achieve better results, but it is more time
 628 consuming compared with using a dwell time. Preparation
 629 time is needed to acquire training data for all stimulus
 630 frequencies. Recognition accuracy was higher than 83%
 631 when using a dwell time in experiments. And there is no
 632 extra time needed in advance. That is an advantage of using a
 633 dwell time. However, a longer dwell time leads to delay of
 634 recognition. In real applications, the choice of the dwell time
 635 should be considered based on requirements of the detection
 636 speed and the detection accuracy.

637 **Table 7** Recognition rates with a threshold during the second session
 638 in the synchronous mode
639

Conditions*	A02	A04	A06	A08
1	0.8468	0.8468	0.8378	0.8739
2	0.8559	0.7658	0.8739	0.8739
3	0.9640	0.9820	1.0000	0.9820

640 *Condition 1: data length=400, overlapping =50%; number of
 641 channels=4; 3 consecutive decisions (overlapping: 2) made one final target
 642 choice;

643 Condition 2: data length=400, overlapping =50%; number of
 644 channels=4; a threshold made one final target choice;

645 Condition 3: data length=400, overlapping =50%; number of
 646 channels=4; a threshold and 2 consecutive decisions (overlapping: 1) made
 647 one final target choice.

648 4.4 Multi-target Recognition

649 **Table 8** Recognition rates under different conditions during all sessions in
 650 the synchronous mode[24]
651

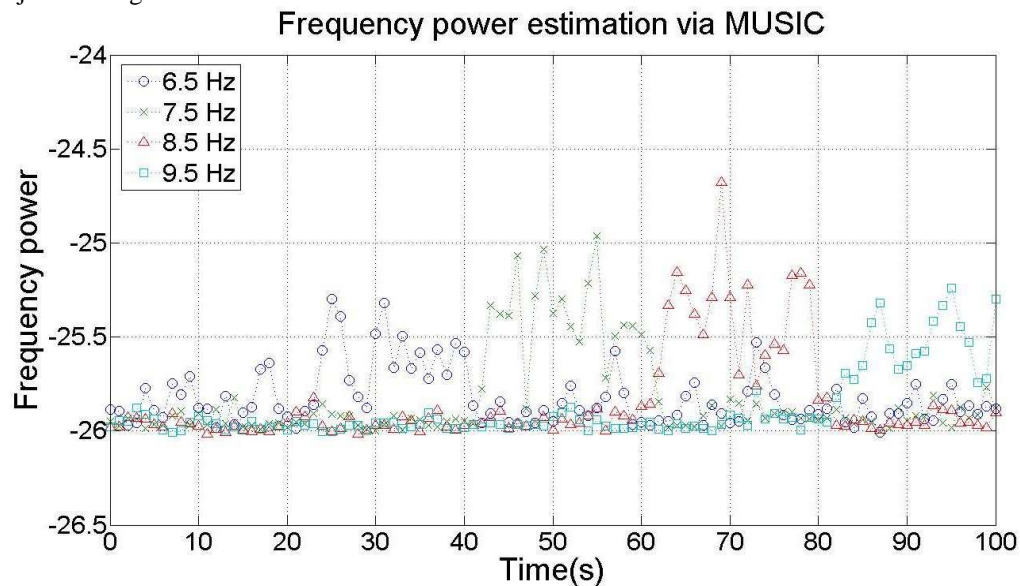
A01	MUSIC	0.7869	A06	MUSIC	0.8378
	CCA	0.7705		CCA	0.7748
A02	MUSIC	0.8468	A07	MUSIC	0.9180
	CCA	0.8649		CCA	0.8852
A03	MUSIC	0.7705	A08	MUSIC	0.8739
	CCA	0.7377		CCA	0.8198
A04	MUSIC	0.8468	B01	MUSIC	0.716
	CCA	0.8649		CCA	0.7284
A05	MUSIC	0.7869	B02	MUSIC	0.6914
	CCA	0.6885		CCA	0.6914

652
653 Table 3 reflects the recognition accuracy when subjects
 654 looked at each stimulus consecutively when all stimuli were

655 flickering. The influence of stimulation design on
 656 recognition results was tested in experiments. If two
 657 neighboring stimuli were too close, it was not easy for
 658 subjects to focus on one stimulus. This explained the poor
 659 results. Through experiments, a distance of 4 cm seemed
 660 reasonable. The distance made the stimulation panel not too
 661 big, and the mutual influence of nearby stimuli could be
 662 reduced. Also, a layer of thin paper was covered on the
 663 stimuli, which made the light more centralized. Recognition
 664 rates shown in Table 3 proved that it did improve the
 665 recognition results.

666 The idle state data and the work state data were analyzed
 667 alone with or without the use of a dwell time as discussed
 668 above. In real applications, all data should be processed
 669 under the same condition. Table 8 shows the recognition
 670 results of one subject during all three sessions. Three

671 consecutive decisions with 2/3 overlapping made a final
 672 target choice. It is shown in Table 8 that the recognition rates
 673 in the work state were reduced compared with the situation
 674 when no dwell time was used. Subjects might have difficulty
 675 in keeping focusing on one stimulus for 40 seconds. This
 676 affected the overall recognition accuracy. For the third
 677 session, the results became even worse. This is mainly
 678 caused by the transition from looking at one stimulus to
 679 looking at another, as seen in Fig. 9 showing the stimulus
 680 frequency power values of data B02 in Table 8. It took time
 681 for subjects to get used to another stimulus. The response
 682 time made the results worse. In addition, 80 seconds was
 683 quite a long time for subjects to keep focused during this
 684 session. The results could be affected if subjects' attention
 685 was distracted.



686 **Fig. 9** Frequency power estimation corresponding to dataset B02
 687
 688

689 4.5 Asynchronous Mode Target Recognition

690 In the asynchronous mode, from both Fig. 7 and Table 4, it
 691 can be estimated that it took about 5 seconds to finish
 692 one-target recognition. But the consumption time is different
 693 for different subjects or sequences. Actually the original data
 694 were processed every one second, but subjects couldn't
 695 move eyes from one stimulus to another instantly. The
 696 response time existed inevitably when subjects were
 697 informed to look at the next stimulus. At most times, one
 698 response potential was evoked following a former potential
 699 quickly. However, for each potential, it lasted for a period of
 700 time. Also, a dwell time caused the delay of one final
 701 decision, which made the whole procedure longer.

702 In the second session, the accuracy when subjects looked
 703 at stimuli as they wanted for about 100 seconds was tested.
 704 The performance was quite good as seen in Table 5. Three of
 705 them achieved accuracy of 100%. For this experiment, not
 706 only the target stimulus should be recognized, but also the
 707 idle state had to be detected. For all experiments in the
 708 asynchronous mode, a dwell time was used to reduce false

709 positives. In addition, the idle state detection was conducted
 710 in this asynchronous mode. All stimuli were flickering and
 711 the subject looked other places rather than the stimulation
 712 panel for 100 seconds. However, in the previous
 713 synchronous mode, only one of the stimuli was on and the
 714 subject looked at other stimuli areas even they were not
 715 flickering. This test in the asynchronous mode means
 716 subjects are completely in an idle state without any external
 717 interference. The recognition accuracy for this experiment is
 718 shown in the following Table 9.

719
 720

Table 9 Idle state detection in the asynchronous mode

Subjects	Accuracy	Total time (seconds)
Subject 1	0.9303	100
Subject 2	0.9055	100
Subject 3	0.9950	100
Subject 4	0.8905	100
Subject 5	0.9876	100

721
 722

It can be seen from Table 9 that the accuracy is better in

723 this experiment than that in the synchronous mode for idle
 724 state detection. The subjects kept in an idle state for a period
 725 of 100 seconds, and the detection accuracy for **Subject 3**
 726 even up to 99.50%, which is a satisfactory result. For in this
 727 experiment, although all stimuli were flickering, the subject
 728 looked at other areas rather than the stimuli. While for the
 729 previous one, the flickering stimulus had influence when
 730 subjects looked at other stimuli areas. Also, no predefined
 731 time duration was set in the asynchronous mode. All these
 732 contributed to good results.

733 4.6 Number of Eigenvectors Constituting the Signal
 734 Subspace

735
 736

Table 10 Recognition rates when p is a constant or adjustable

Data	p: constant	p: adjustable
A01	0.5372	0.5372
A02	0.9095	0.9457
A03	0.6529	0.7438
A04	0.9231	0.9819
A05	0.6033	0.6529
A06	0.9548	0.9593
A07	0.8430	0.8512
A08	0.9186	0.9276

737

738 It was mentioned that a segmentation ratio was proposed
 739 to confirm the number of eigenvectors to be used for
 740 constituting the signal subspace of the MUSIC method in our
 741 research. This value can be set to a constant, too. Let p
 742 represent this value. We did experiments to compare the
 743 recognition results as shown in Table 10 by using the

744 constant method and the proposed method.

745 Table 10 reflects that the proposed method produced
 746 better results. It is more flexible than the constant method.
 747 However, the segmentation ratio is set to be 0.01 in our
 748 research. This ratio was obtained after conducting some
 749 previous data analysis, too.

750 4.7 Control of a Virtual Keyboard

751 Fig. 10 illustrates the power values corresponding to five
 752 stimuli. The five frequencies are 6.5, 7, 7.5, 8 and 8.5 Hz,
 753 which are mapped to five numbers 1, 2, 3, 4 and 5. The
 754 numbers are used to represent five commands: up, confirm,
 755 left, down and right.

756 As seen in Fig. 10, the frequency corresponding to the
 757 maximum power value is different during the spelling
 758 process. The number sequence is “4-5-2-4-2-3-3-2-1-2-3-2”
 759 when mapping the frequencies to numbers. This sequence is
 760 translated to commands
 761 “up-right-confirm-down-confirm-left-left-confirm-up-confir
 762 m-left-confirm”. According to these commands, five letters
 763 B, R, A, I and N are selected. It takes about 60 seconds to
 764 finish the whole procedure, which means each step
 765 consumes about 5 seconds. It is noticed that a control
 766 strategy was used during the spelling procedure. Only if one
 767 recognition number (corresponding to one frequency target)
 768 lasts for a certain period of time, is a control command
 769 confirmed. This explains the recognition time is longer than
 770 that of the asynchronous mode experiments without device
 771 control, too. If the commands change too quickly, the cursor
 772 moves quickly. It is hard for subjects to focus on one letter or
 773 symbol. Also, the subjects need time to decide the move path
 774 of the cursor. This is why the control strategy is necessary.
 775

Frequency power estimation via MUSIC

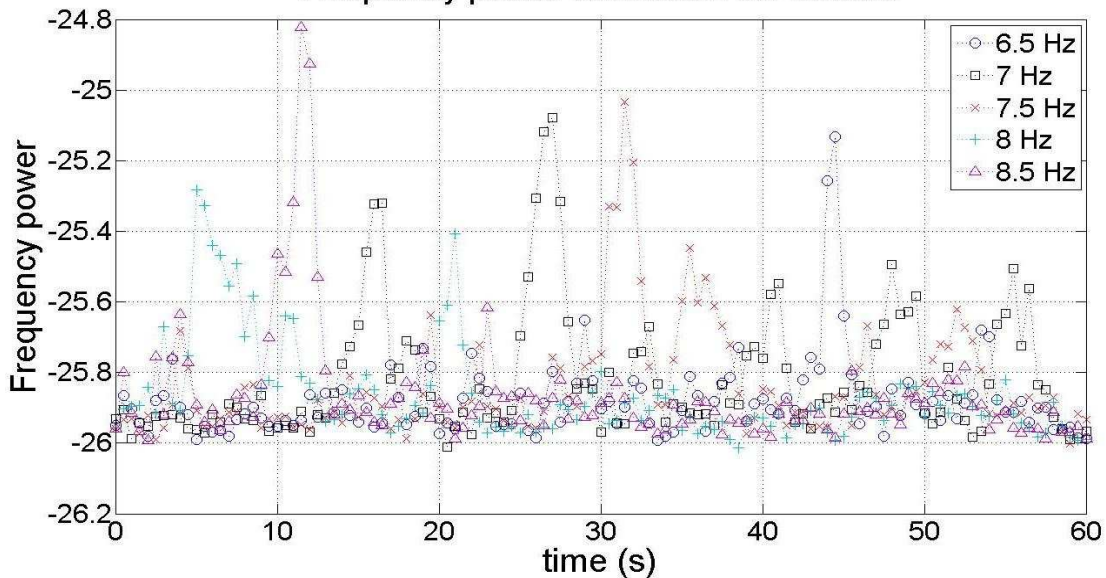


Fig. 10 Frequency power values during the process of spelling “BRAIN”

776
 777
 778

779 5 CONCLUSIONS

780 SSVEP-based BCI systems have great potential in real

781 world applications, and the signal processing algorithm is of
 782 great importance. In this paper, a MUSIC-based method was
 783 proposed for multi-dimensional signal processing and a

784 segmentation ratio for determining the number of
 785 eigenvectors constituting the signal subspace was suggested.
 786 The experimental results with simulated data proved that
 787 this method could provide high frequency resolution. Also,
 788 the multi-channel(dimensional) signals have the anti-noise
 789 ability, so the power spectrum estimation is more accurate.
 790 The method was verified with real SSVEP signals
 791 acquired in an unshielded environment. The original data
 792 were segmented into 2-second epochs with a sampling
 793 frequency of 200 Hz. Four channels were enough for feature
 794 extraction. The basic idea was to compute the frequency
 795 power at stimulus frequencies. Then the frequency with the
 796 maximum power value was recognized as the target one. The
 797 results showed targets could be well recognized either one
 798 stimulus was on or all stimuli were on, compared with a
 799 typical multi-channel signal processing method CCA. It was
 800 feasible to detect the idle state using a dwell time in our
 801 experiments. A disadvantage of this method is that it caused
 802 time delay for each decision. An alternative way is to use a
 803 threshold, which was obtained with training data. In our
 804 research, the threshold was gradually adjusted to maximize
 805 the overall recognition accuracy of the training data. Though
 806 it didn't cause recognition delay, the preliminary time was
 807 longer.
 808 Finally, the proposed method was implemented in a real
 809 time application of keyboard control. Different subjects
 810 could use the virtual keyboard successfully.
 811 Future work includes improving the algorithm to
 812 recognize the target within less time and with higher
 813 accuracy. Other factors like design of the stimuli, the
 814 subjects comfort, all should be taken into account to develop
 815 practical applications for disabled people.

816 ACKNOWLEDGEMENTS

817 This work was supported by the National Science
 818 Foundation (Grant No. 51475342). The authors would like to
 819 thank all subjects for their participating in the experiments.

820 REFERENCES

821 1. Wolpaw JR, Birbaumer N, Heetderks WJ, McFarland DJ,
 822 Peckham PH, Schalk G, Donchin E, Quatrano LA,
 823 Robinson CJ, Vaughan TM (2000) Brain-computer
 824 interface technology: A review of the first international
 825 meeting. *IEEE Trans. Rehabil. Eng.* 8 (2):164-173
 826 2. Mason SG, Birch GE (2003) A general framework for
 827 brain-computer interface design. *IEEE Trans. Neural
 828 Syst. Rehabil. Eng.* 11 (1):70-85
 829 3. Wang Y WR, Gao X (2006) A practical VEP-based
 830 brain-computer interface. *IEEE Trans. Neural Syst.
 831 Rehabil. Eng.* 14 (2):234-240
 832 4. Picton T (1990) Human brain electrophysiology: evoked
 833 potentials and evoked magnetic fields in science and
 834 medicine. *J. Clin. Neurophysiol.* 7:450-451
 835 5. Bin GY, Gao XR, Yan Z, Hong B, Gao SK (2009) An
 836 online multi-channel SSVEP-based brain-computer
 837 interface using a canonical correlation analysis method.
 838 *J. Neural Eng.* 6 (4):1-6(046002)

839 6. Liu Q, Chen K, Ai Q, Xie SQ (2014) Review: Recent
 840 Development of Signal Processing Algorithms for
 841 SSVEP-based Brain Computer Interfaces. *J. Med. Biol.
 842 Eng.* 34 (4):299-309
 843 7. Muller-Putz GR, Pfurtscheller G (2008) Control of an
 844 electrical prosthesis with an SSVEP-based BCI. *IEEE
 845 Trans. Biomed. Eng.* 55 (1):361-364
 846 8. Bian Y, Li HW, Zhao L, Yang GH, Geng LQ (2011)
 847 Research on steady state visual evoked potentials based
 848 on wavelet packet technology for brain-computer
 849 interface. *Proc. Eng.* 15:2629-2633
 850 9. Zhang Z, Li X, Deng Z (2010) A CWT-based SSVEP
 851 classification method for brain-computer interface
 852 system. In: *International Conference on Intelligent Control
 853 and Information Processing*, pp 43-48
 854 10. Yan B, Li Z, Li H, Yang G, Shen H (2010) Research on
 855 brain-computer interface technology based on steady
 856 state visual evoked potentials. In: *4th International
 857 Conference on Bioinformatics and Biomedical
 858 Engineering*, pp 1-4
 859 11. Wu CH, Chang HC, Lee PL, Li KS, Sie JJ, Sun CW,
 860 Yang CY, Li PH, Deng HT, Shyu KK (2011) Frequency
 861 recognition in an SSVEP-based brain computer interface
 862 using empirical mode decomposition and refined
 863 generalized zero-crossing. *J. Neurosci. Methods* 196
 864 (1):170-181
 865 12. Wu CH, Chang HC, Lee PL (2009) Instantaneous
 866 gaze-target detection by empirical mode decomposition:
 867 application to brain computer interface. In: *World
 868 Congress on Medical Physics and Biomedical
 869 Engineering*, pp 215-218
 870 13. Friman O, Luth T, Volosyak I, Graser A (2007) Spelling
 871 with steady-state visual evoked potentials. In: *3rd
 872 International IEEE/EMBS Conference on Neural
 873 Engineering*, pp 354-357
 874 14. Volosyak I (2011) SSVEP-based Bremen-BCI interface -
 875 boosting information transfer rates. *J. Neural Eng.* 8
 876 (3):1-11(036020)
 877 15. Volosyak I, Malechka T, Valbuena D, Graser A (2010) A
 878 novel calibration method for SSVEP based
 879 brain-computer interfaces. In: *18th European Signal Proc.
 880 Conf.*, pp 939-943
 881 16. Cecotti H (2010) A self-paced and calibration-less
 882 SSVEP-based brain-computer interface speller. *IEEE
 883 Trans. Neural Syst. Rehabil. Eng.* 18 (2):127-133
 884 17. Zhang ZM, Deng ZD (2012) A kernel canonical
 885 correlation analysis based idle-state detection method for
 886 SSVEP-based brain-computer interfaces. In: *2nd
 887 International Conference on Material and Manufacturing
 888 Technology*, pp 634-640
 889 18. Lin ZL, Zhang CS, Wu W, Gao XR (2006) Frequency
 890 recognition based on canonical correlation analysis for
 891 SSVEP-based BCIs. *IEEE Trans. Biomed. Eng.* 53
 892 (12):2610-2614
 893 19. Hakvoort G, Reuderink B, Obbink M (2011) Comparison
 894 of PSDA and CCA detection methods in a SSVEP-based
 895 BCI-system. *Centre for Telematics and Information
 896 Technology, University of Twente*,
 897 http://eprints.eemcs.utwente.nl/19680/01/Comparison_of_PSDA_and_CCA_detection_methods_in_a_SSVEP-b

899 ased_BCI-system.pdf
900 20. Schmidt RO (1986) Multiple emitter location and signal
901 parameter estimation. IEEE Trans. Antennas Propag. 34
902 (3):276-280
903 21. Swami A, Mendel JM, Nikias CL (1998) Higher-order
904 Spectral Analysis Toolbox: for Use with MATLAB:
905 User's Guide. Mathworks, Incorporated
906 22. Wang Yongliang CH, Peng Yingning, Wan Qun (2004)
907 Theories and algorithms of spatial spectrum estimation.
908 Press of Tsinghua University
909 23. Hardoon D R SS, Shawe-Taylor (2004) Canonical
910 correlation analysis: An overview with application to
911 learning methods. Neural Comput. 16 (12):2639-2664
912 24. Chen K, Liu Q, Ai QS (2014) Multi-channel SSVEP
913 pattern recognition based on MUSIC. In: 4th
914 International Conference on Intelligent Structure and
915 Vibration Control, pp 84-88
916